



## Enhanced gas permeation performance of mixed matrix membranes containing polysulfone and modified mesoporous MCM-41

KAVEH ABBASI KOLOLI<sup>1</sup>, SEYED MOSTAFA TABATABAEE GHOMSHEH<sup>1\*</sup>, MAZIAR NOEI<sup>2</sup> and MASOUD SABERI<sup>3</sup>

<sup>1</sup>Department of Chemical Engineering, Mahshahr Branch, Islamic Azad University, Mahshahr, Iran; <sup>2</sup>Department of Chemistry, Faculty of Pharmaceutical Chemistry, Tehran Medical Sciences, Islamic Azad University, Tehran, Iran; <sup>3</sup>Department of Chemical Engineering, Bushehr Branch, Islamic Azad University, Bushehr, Iran

(Received 19 February, revised 18 April, accepted 29 April 2021)

**Abstract:** The aim of this study was the development of mixed matrix membranes (MMMs) based on silica MCM-41 dispersed in polysulfone (PSf) for the separation of carbon dioxide from methane. For this purpose, MCM-41 was synthesized by a hydrothermal method and was modified with 3-aminopropyltriethoxysilane (APTES). SEM, FTIR, BET and XRD analyses were used for characterization of the modified and unmodified particles. Then, various MMMs containing PSf at different weight percents (5, 10, 15 and 20) of modified and unmodified particles were prepared and the morphology and structure of the prepared membranes were studied using SEM and XRD analyses. Regardless of the particle type, the addition of MCM-41 to PSf caused an increase in gas permeability compared to a neat PSf membrane. Adding unmodified particles to PSf matrix resulted in undesirable effects, including particle agglomeration and/or the formation of interfacial voids. The MMMs with modified MCM-41 showed relatively better separation performance compared to MMMs with unmodified MCM-41. As a result, the MMM of PSf with 20 wt. % modified MCM-41 showed a significant increase in selectivity of carbon dioxide/methane and the value of selectivity reached 25.24.

**Keywords:** PSf; MCM-41; surface modification; silane coupling agent; gas separation.

### INTRODUCTION

Separation of carbon dioxide as an undesirable component for increasing the heating value of fuel is one of the general separation processes in the natural gas industry. Furthermore, carbon dioxide causes corrosion of process equipment in

\* Corresponding author. E-mail: m.tabatabaei@mhria.ac.ir  
<https://doi.org/10.2298/JSC210219034A>

the presence of water. Therefore, the separation of carbon dioxide from methane and bringing it to an acceptable level before the distribution of natural gas is essential.<sup>1–3</sup>

Polymeric membranes are widely used in natural gas separation processes. The difference in gas permeability rates is the basis of membrane processes for the separation of gases.<sup>4–7</sup> Polymeric membranes have good process properties, including low energy consumption, high transport properties, and low current and constant cost. Currently, the membranes have many applications for the separation of gases, such as oxygen/nitrogen enrichment, hydrogen recycling, separation of carbon dioxide from methane or nitrogen, and separation of organic materials from the output currents.<sup>8,9</sup>

Membrane technology for removal of carbon dioxide has been established since the 1980s with the rapid growth of the natural gas industry.<sup>10,11</sup> Robeson reported that there is usually a reverse relationship between permeability and selectivity for neat polymer membranes.<sup>12</sup> To overcome this drawback of neat polymer membranes, mineral fillers with porous structure were used within the polymer matrix to improve the gas separation performance. These minerals have unique structure, surface chemistry and mechanical strength. These compounds, known as MMMs, have been extensively tested for the separation of carbon dioxide from natural gas, Flue gas and biogas.<sup>13–19</sup>

Depending on the type of nanoparticles, MMMs can significantly reduce the cost of membranes in comparison to expensive inorganic membranes.<sup>20,21</sup> The presence of porous silica particles in the polymer matrix with a proper distribution leads to improvement in the mechanical strength and thermal stability of the polymer. High specific surface area, high surface adsorption of carbon dioxide, narrow and regular channels, large pore sizes with adjustable pore dimensions, high thermal and mechanical stability and simplicity of surface modification are the most important characteristics of MCM-41, which makes these nanoparticles known as the most famous member of the M41S family (MCM-41, MCM-48, MCM-50).<sup>22–26</sup> It is worth mentioning that one of the most important criteria in MMMs is the achievement of good adhesion between the mineral filler and the polymer matrix. Generally, glassy polymers have good separation performance and high mechanical stability. However, the use of some polymers to fabricate a MMM due to the lack of suitable compatibility between the surface of inorganic nanoparticles and polymer matrix may have non ideal effects, such as agglomeration of the particles and formation of surface voids around the particles. These defects, which cause non selective voids in the membrane, are the most important challenges in the fabrication of an MMM.<sup>27,28</sup> Sorribas *et al.* investigated the effect of adding micro-mesoporous silica ZIF-8 -MSS to the PSf matrix for the separation of carbon dioxide/methane. They reported that in the fabricated membrane, gas permeability increased and selectivity was almost

unchanged.<sup>29</sup> One of the most important points in the preparation of MMMs is the homogeneous dispersion of particles in the polymer matrix, which has a direct effect on the properties of the MMMs.<sup>30</sup> Vankelecom *et al.* improved the compatibility between the nanoparticles and the polymer matrix by modifying the outer surface of the zeolite. As a result, the prepared membrane showed better performance under optimal conditions of silane use.<sup>31</sup>

In the present research, silica MCM-41 was synthesized by the hydrothermal method and the solvent method (SO) was used for modifying the particles employing the APTES silane coupling agent. Modified and unmodified particles were characterized by SEM, FTIR and XRD analyses. Then, three groups of membranes, including neat PSf membrane, MMMs consisting of PSf and different content (5, 10, 15, 20 wt. %) of unmodified and APTES-modified MCM-41 were prepared, which were labelled as PSf, PSf-UMO-Mx and PSf-AP-Mx ( $x$  indicates the weight percentage of particles). These membranes were examined by XRD and SEM analyses. Finally, the performance of these membranes in the separation of carbon dioxide from methane was studied by gas permeability and selectivity tests.

## EXPERIMENTAL

### Materials

Cetyltrimethylammonium bromide (CTAB), tetraethylorthosilicate (TEOS), sodium hydroxide (NaOH), tetrahydrofuran (THF) and APTES were purchased from Merck. Anhydrous toluene was purchased from Sigma Chemical Co. Moreover, polysulfone (Udel P-1700 grade), a glassy polymer with a glass transition temperature ( $T_g$ ) of 185 °C, was obtained from Amoco.

### Synthesis and Functionalization of MCM-41 mesoporous silica

*Synthesis of MCM-41 particles.* The hydrothermal method was used to achieve MCM-41 particles with a uniform pore size distribution.<sup>32,33</sup> In this method, an aqueous micellar solution containing 1 g of CTAB surfactant, 0.28 g of sodium hydroxide and 480 ml of deionised water was prepared under stirring for 1 h. Then, 5 ml of TEOS, as a silica source, was slowly added to the solution at 80 °C in an oil bath to form a white slurry solution. After 2 h stirring (500 rpm), the slurry was transferred to a glass container and was left for 24 h to be completely transformed. The slurry was filtered using a ceramic filter and washed many times with deionised water until the filtrate became neutral. Then, the resulting precipitate was dried at ambient temperature. Finally, the obtained powder was calcined at 550 °C in air for 6 h to remove the surfactant.

*Functionalization of MCM-41 particles.* The synthesized MCM-41 particles were silylated as follows: in the first step, 100 ml of toluene and 0.4 g of MCM-41 were mixed and this mixture was sonicated for 5 min. Then 0.4 g of APTES was dissolved in the toluene and the suspension solution was refluxed at 68 °C for 6 h under nitrogen atmosphere to form covalent bond between functional components and particle surface. After cooling, the mixture was filtered using filter paper. Finally, the excess amine was removed by Soxhlet extraction for 10 h using dichloromethane and the amine modified MCM-41 particles were dried for 6 h at room temperature under vacuum.

### *Fabrication of membranes*

The neat membrane and MMMs were fabricated using the solution casting method. Before preparation of the membranes, PSf was degassed at 80 °C for 8 h under vacuum to remove absorbed moisture. For preparing the neat membrane with 10 wt. % PSf, 0.5 g PSf was added to 4.5 g THF and stirred at room temperature to obtain a uniform solution. Then, the preparation solution was cast on a glass plate and placed at 40 °C for 24 h to evaporate the solvent. The remaining solvent in the prepared membrane was evaporated in a vacuum oven at 85 °C for 4 h.

For fabrication of the MMMs, in the first step, due to the presence of different number of particles in the polymer matrix (5, 10, 15 and 20 wt. %), the amount of each modified and unmodified MCM-41 was dried in a vacuum oven. Then, the fillers were added to 3 g of THF and the mixture was stirred for 10 h and to increase dispersion was sonicated for 20 min. The process of stirring and sonicating were repeated twice. At the same time, a homogeneous solution containing PSf and THF was stirred in another container. Then 4–5 drops of this solution were added to the suspension and this suspension was stirred and sonicated for 20 min again in order to cover the surface of the particles. Then, the remainder of the polymeric solution was added to the suspension and this suspension was stirred and sonicated to prevent formation of particle agglomerates. Then, the mixture was stirred for 4 h at room temperature and was sonicated for 10 minutes to remove any gas bubbles before casting. The final casting on a glass plate was similar to that used for the neat PSf membrane.

### *Characterization*

Fourier transform infrared (FTIR) spectroscopy was performed using a Thermo Avatar spectrometer in the range of 4000–400 cm<sup>-1</sup> to characterize the functional groups of the particles. The morphology of unmodified and modified MCM-41 particles and membranes was investigated using a MIRRA 3 Tescan scanning electron microscope (SEM). The N<sub>2</sub> adsorption–desorption isotherms were collected at 77 K using Micromeritics ASAP 2020. The Surface areas and the pore size distribution were determined by the BET and BJH methods, respectively. Membranes were broken under liquid nitrogen and sputter coated with gold using Cressington HR208 (UK) high resolution sputter coater. X-Ray diffraction (XRD) patterns were determined using a X'Pert Pro, analytical X-ray diffractometer. The results were recorded using Cu K $\alpha$  radiation ( $\lambda = 0.154$  nm) in the  $2\theta$  range of 1–10° for MCM-41 and in the  $2\theta$  range of 10–90° for the neat membrane and MMMs.

### *Gas permeation measurements*

The permeability in the neat membrane and MMMs fabricated using the constant pressure method was measured with a soap bubble flow-meter. The gas permeability device consisted of a gas permeability cell in which the membrane is placed and one side is exposed to the gas feed. The pressure on the feed side was regulated by a regulator and measured by a pressure gauge. In this study, the fabricated membranes were tested for gas permeability to methane and carbon dioxide gases with a purity of 99.99 %.

The permeability of gas *i* in the membrane,  $P_i$ , is obtained using Eq. (1):

$$P_i = \frac{l}{A\Delta p} \frac{dV_i}{dt} \quad (1)$$

where  $P_i$  / Barrer is the permeability of gas *i* (1 Barrer = 10<sup>-10</sup> cm<sup>3</sup><sub>STP</sub> cm<sup>-2</sup> s<sup>-1</sup> cmHg<sup>-1</sup>);  $V_i$  / cm<sup>3</sup> is the volume of displaced gas in the soap bubble flow-meter or volume of gas permeation in the membrane;  $A$  / cm<sup>2</sup> is the effective surface area of the membrane;  $l$  / cm is the thickness of the

membrane, which was measured with a micrometer;  $t$  / s is the time interval of soap bubble movement in the column and  $\Delta p$  is the pressure drop across the membrane, cm<sub>Hg</sub>. The gas permeability in this study was determined at a pressure of 8 bar.

The ideal selectivity of gases,  $\alpha_{ij}$ , for each membrane was obtained with Eq. (2):

$$\alpha_{ij} = \frac{P_i}{P_j} \quad (2)$$

where  $\alpha_{ij}$  is the ideal selectivity of gas  $i$  to  $j$  and  $P_i$  and  $P_j$  are the permeability of the gases  $i$  and  $j$ , respectively.

## RESULTS AND DISCUSSION

### *Characterization results of silica MCM-41*

The particles morphology was assessed by SEM analysis. SEM images of the unmodified MCM-41 particles and the particles modified with APTES are shown in Fig. 1. Unmodified MCM-41 particles (Fig. 1a) have particle diameters of about 200 to 650 nm and a spherical shape. The modified MCM-41 particles (Fig. 1b) have diameters in the range of 200 to 650 nm and a spherical shape. As can be seen, the MCM-41 particles did not undergo structural and morphological changes after modification, and their structure was preserved.

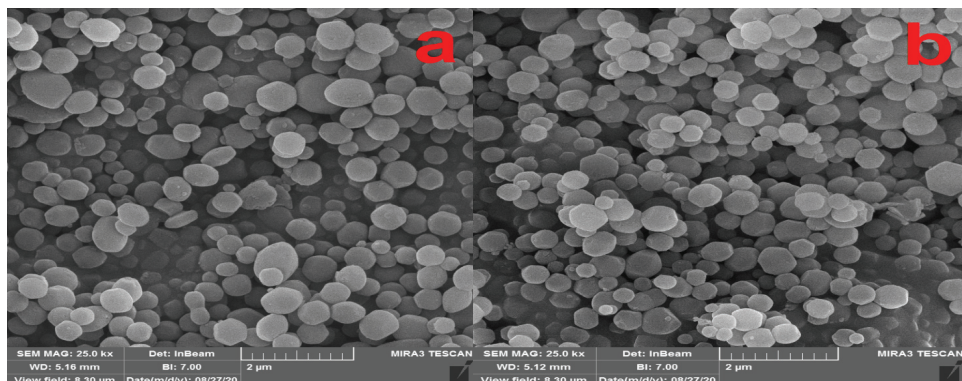


Fig. 1. SEM image of: a) unmodified and b) APTES modified MCM-41.

The infrared spectra of MCM-41 in the range 4000–400 cm<sup>-1</sup> before and after functionalization with APTES are shown Fig. 2. The inset of the figure shows the clarification of peaks in the range of 1250–400 cm<sup>-1</sup>. As shown in Fig. 2a, for unmodified MCM-41 particles, the peaks observed in region 3402 cm<sup>-1</sup> are due to O–H stretching vibrations of water molecules adsorbed on its surface as well as hydroxyl silanol groups Si–OH. The peak observed at 1626 cm<sup>-1</sup> belongs to the vibrations of H<sub>2</sub>O molecules trapped in the lattice. The main characteristic of MCM-41 particles is the presence of a silicate network. This characteristic is observed by the peaks at 460, 950 and 1084 cm<sup>-1</sup>, which belong to the Si–O–Si, Si–OH and Si–O silicate groups, respectively. As can be seen in

Fig. 2b, a new peak appeared in the  $2932\text{ cm}^{-1}$  region after APTES functionalized the mesoporous silica particles. This peak belongs to the vibrations of C–H groups, which are caused by the substituent propyl group of APTES. The changes observed in the  $1480\text{ cm}^{-1}$  region also indicate changes in amine bonds that occur after functionalization of the particles. Amination also changes the appearance of the peak at  $3402\text{ cm}^{-1}$ . The above observations show that modification of particles was successfully performed by APTES using the SO method.

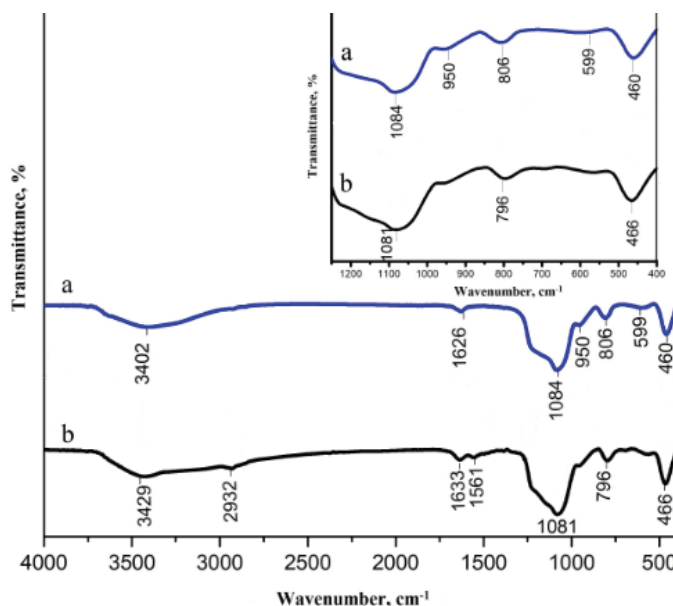


Fig. 2. FTIR spectra for the unmodified (a) and APTES modified (b) MCM-41.

The XRD spectrum for unmodified MCM-41 particles is shown in Fig. 3. The diffraction angles observed at  $2\theta$   $1.75$ ,  $3.65$ ,  $4.3$  and  $5.9^\circ$  belong to the (100), (110), (200) and (210) planes, respectively. These peaks are well matched to the hexagonal P6 space array of MCM-41 particles<sup>32</sup> and indicate the crystallinity of silica MCM-41 particles. Since MCM-41 is not crystalline at the atomic level, no reflection were observed at higher angles. The results indicate the MCM-41 particles were successfully synthesized.

The specific surface area (SBET) and average pore diameter ( $Pd$ ) of unmodified and modified MCM-41 particles are presented in Table I and Fig. 4. In addition, pore diameter ( $D$ ) and pore volume ( $v$ ) are shown in Fig. 4. The inset of the Figure shows the pore size diameter of unmodified and modified MCM-41 particles. Nitrogen adsorption isotherms at  $77\text{ K}$  for unmodified and modified MCM-41 both are reversible type IV adsorption isotherms corresponding to a mesoporous material. Unmodified MCM-41 particles had a specific surface area

of  $1111.6 \text{ m}^2 \text{ g}^{-1}$ , while after modification, the specific surface area of the particles decreased to  $520.52 \text{ m}^2 \text{ g}^{-1}$  due to functionalization using APTES. The pore size distribution was computed using the BJH method.

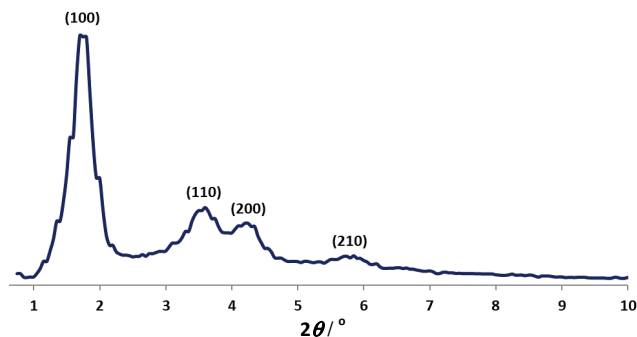


Fig. 3. XRD pattern of unmodified MCM-41.

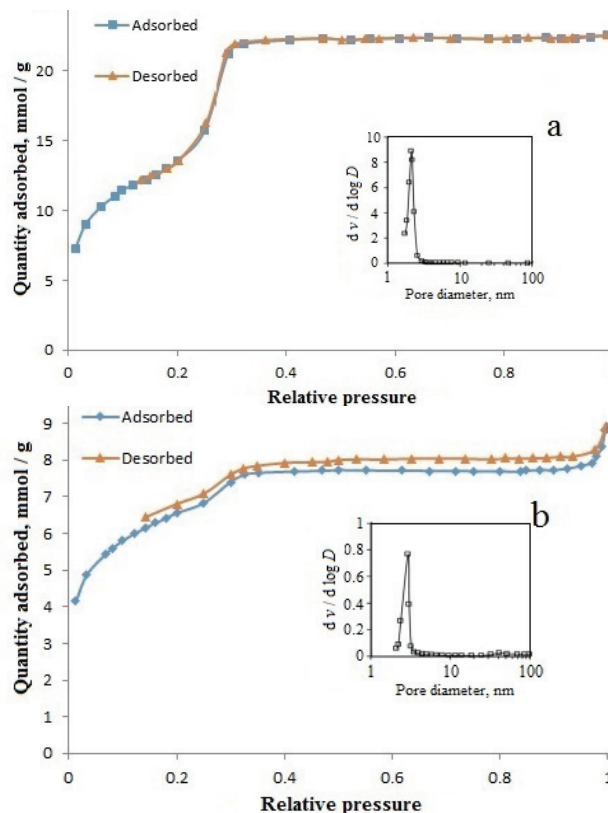


Fig. 4. BET isotherms and BJH pore size distribution for the unmodified (a) and the APTES-modified (b) MCM-41.

TABLE I. Specific surface area and average pore diameter of MCM-41 before and after modification

Type of silica MCM-41	Surface modified MCM-41 materials	$S_{BET} / \text{m}^2 \text{ g}^{-1}$	$D_p / \text{nm}$
Unmodified MCM-41	—	1111.6	2.88
Modified MCM-41	APTES	520.52	2.61
Unmodified MCM-41 <sup>25</sup>	—	845	3.1
Modified MCM-41*	<i>n</i> -Octyldimethylmethoxysilane	528	2.3

The average pore diameter of 2.88 nm for unmodified particles was obtained. Also, it was observed that the diameter of the pores remains almost in the same range after functionalization and reach to 2.61 nm that shows the mesoporous structure was preserved. According to Table I and Fig. 4, the decrease in surface area and average pore diameter showed the presence of APTES on the surface of MCM-41.

#### *Characterization results of mixed matrix membranes*

SEM images of the cross section for neat PSf membrane and PSf-UMO-M10 MMM are shown in Fig. 5. As can be seen in Fig. 5a, the cross-sectional SEM image of the neat PSf membrane shows a homogeneously dense morphology while dispersion of the unmodified MCM-41 particles in the MMM increases the roughness of the cross section. Fig. 5b shows the agglomeration of particles and the presence of surface voids in the surface between the polymer and the particle.

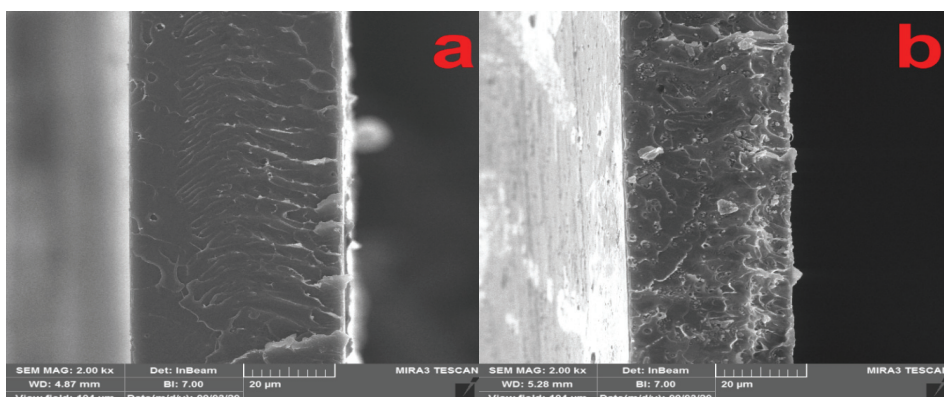


Fig. 5. SEM images of cross section of: a) neat PSf membrane and b) PSf-UMO-M10 MMM.

The results of XRD analysis for the neat PSf membrane, PSf-UMO-M10 and PSf-AP-M10 MMMs are shown in Fig. 6. As can be seen, the neat PSf membrane has an amorphous structure with a large peak at  $2\theta = 18^\circ$  and a small peak around  $2\theta = 44^\circ$ . The XRD pattern of different MMMs shows peaks similar to those for neat PSf originating from the amorphous polymer structure. Therefore, the addition of MCM-41 silica particles to PSf did not change the diffraction pattern of PSf

membrane and the pattern characteristic and amorphous characterization of the membrane were preserved. It should be noted that crystalline phases are considered as impermeable regions and the permeability of gas from semi-crystalline polymer membranes is much lower than from amorphous polymer membranes due to the reduction of space for the diffusion of gases as a result of the winding path around the crystals.<sup>28</sup>

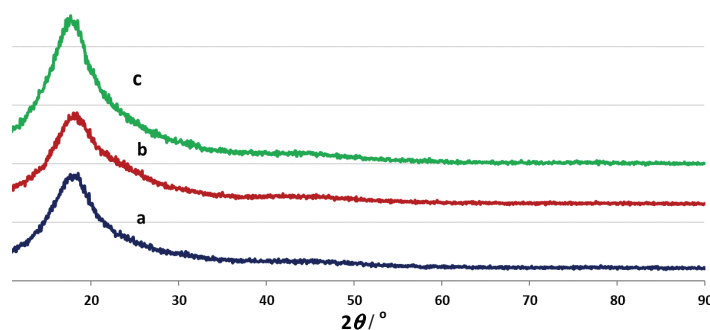


Fig. 6. XRD patterns for: a) the neat PSf, b) PSf-UMO-M10 and c) PSf-AP-M10.

#### *Gas separation results*

Gas separation properties including carbon dioxide and methane permeability and ideal selectivity of carbon dioxide/methane for neat PSf membrane and PSf-modified and unmodified MCM-41 MMMs are given in Figs. 7 and 8. In addition, the effect of the presence of different types of MCM-41 (20 wt. %) in the MMMs on the permeability and selectivity is given in Table II.

Regardless of the type of particles (modified and unmodified particles), the addition of MCM-41 to the PSf matrix increased the permeability of all MMMs in comparison to the neat PSf membrane. In general, this increase in permeability in fabricated MMMs has two main reasons: one is that the addition of filler particles increases the volume of voids in the polymer and the other is that the inherent permeability of fillers is higher than that of the polymer. On the other hand, the increase in selectivity in the MMMs fabricated of PSf and modified MCM-41 particles is due to the proper performance of APTES, which allows carbon dioxide to pass through the membrane more easily than methane.<sup>34</sup>

In the PSf-unmodified MCM-41 MMM up to 10 wt. %, the selectivity increased slightly and at higher concentrations decreased (Fig. 8). The reason for this decrease in selectivity is probably related to the low quality of particles dispersion and the formation of non-selective voids in the PSf matrix. The agglomeration of unmodified particles in the polymer matrix is due to the hydroxyl-hydroxyl attraction, which causes improper particles dispersion and reduces the effect of the MCM-41 molecular sieving mechanism.<sup>27</sup>

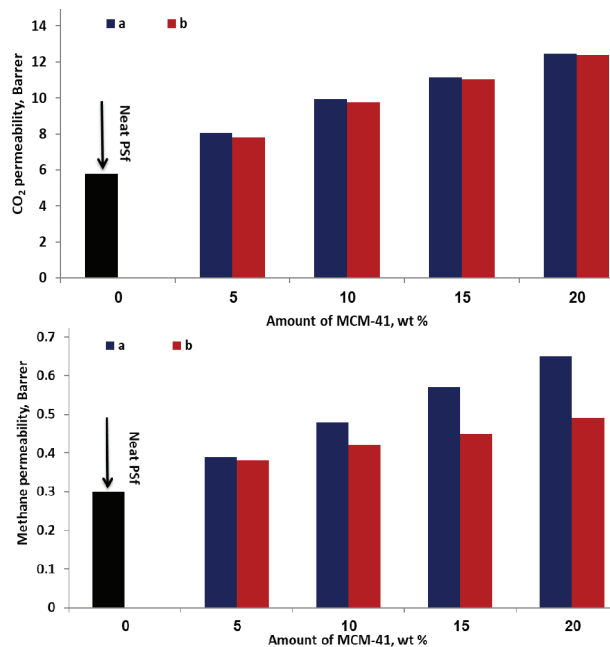


Fig. 7. Effect of: a) unmodified and b) APTES-modified MCM-41 loading on the measured permeabilities of carbon dioxide (left side) and methane (right side) through MMMs at 8 bar and room temperature.

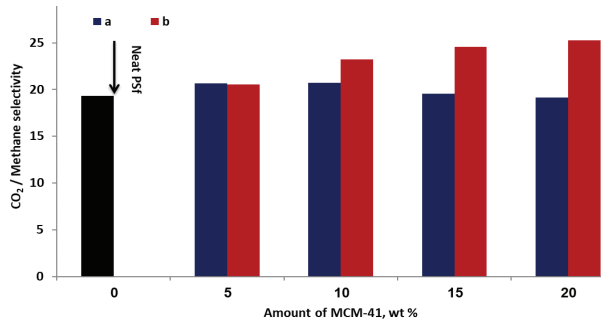


Fig. 8. Effect of: a) unmodified and b) APTES-modified MCM-41 loading on the carbon dioxide/methane selectivity for MMMs at 8 bar and room temperature.

In MMMs consisting of mineral particles dispersed in a polymer matrix, the bond between the two materials plays an important role in the performance of these membranes. A silane coupling agent can increase the adhesion between a polymer matrix and mineral fillers.<sup>35</sup> Therefore, in order to increase the adsorption capacity of carbon dioxide by the membrane, the surface of silica MCM-41 particles was modified before being placed in the polymer matrix by APTES and its effect on the separation performance of PSf-MCM-41 MMM was investigated. For APTES-

-modified particles in the PSf matrix, the polar groups of the aminopropyl bond interact with the polar sulfone groups to form new hydrogen bonds. Therefore, the addition of modified MCM-41 particles to PSf causes the particles to be homogeneously dispersed in the polymer structure and produce a MMM without defects. Under these conditions, even at high weight percentages, the particles disperse properly and increase the selectivity of MMMs.

TABLE II. Permeabilities and selectivity's of carbon dioxide and methane through the unmodified and modified MCM-41 (20 wt. %) MMMs at 8 bar and room temperature

Membrane	$P_{\text{CO}_2}$ / Barrer	$P_{\text{methane}}$ / Barrer	$\alpha = P_{\text{CO}_2}/P_{\text{methane}}$
PSf-UMO-M20	12.46	0.65	19.17
PES-UMO-M20 <sup>27</sup>	3.56±0.17	0.13±0.01	26.5
PSf-AP-M20	12.37	0.49	25.24
PES-APTMS-M20 <sup>27</sup>	3.44±0.16	0.1±0.01	35.6

The addition of the unmodified MCM-41 to the PSf matrix caused a significant increase in membrane permeability compared to other fabricated membranes (Fig. 7). As a result, the highest permeability was obtained for the PSf-UMO-M20 MMM, in which the permeability of carbon dioxide increased by 114.83 % compared to neat PSf membrane. The selectivity of carbon dioxide/methane in the PSf-AP-M20 MMM compared to neat PSf membrane showed a significant increase and reached 25.24 from 19.33.

#### CONCLUSIONS

In this work, silica MCM-41 was successfully synthesized by a hydrothermal method and a solvent method was used for modifying these particles by using an APTES silane coupling agent. Modified and unmodified particles were characterized by SEM, FTIR and XRD analyses. Then, three groups of membranes including neat PSf, MMMs consisting of PSf and different weight fractions (5, 10, 15 20 %) of modified and unmodified MCM-41 were prepared and the performance of these membranes in the separation of carbon dioxide from methane was studied by gas permeability and selectivity tests. The results show an increase in the permeability by adding MCM-41 into the PSf matrix, although depending on the modification of MCM-41 using silane coupling agent, the selectivity showed different trends. Due to the tendency of unmodified particles to form hydrogen bonds, particles agglomeration occurs in the polymer matrix at high loading that form non-selective voids. As a result, in MMMs fabricated with unmodified particles, the ideal selectivity did not change much compared to neat PSf membrane. For MMMs with modified MCM-41, the surface modification prevented the formation of hydrogen bonds between particles due to the long side chains of APTES. Moreover, APTES bonding groups have a good compatibility with the polymer matrix even at high loadings (up to 20 wt. %). Therefore, the selectivity

of carbon dioxide/methane was significantly increased compared to the MMMs comprising unmodified MCM-41.

#### ИЗВОД

### ПОБОЉШАЊЕ ПЕРФОРМАНСЕ МЕШАНИХ МАТРИЧНИХ МЕМБРАНА КОЈЕ САДРЖЕ ПОЛИСУЛФОН И МОДИФИКОВАНИ МЕЗОПОРОЗНИ МСМ-41 ЗА ПРОПУШТАЊЕ ГАСА

KAVEH ABBASI KOLOLI<sup>1</sup>, SEYED MOSTAFA TABATABAEI QOMSHEH<sup>1</sup>, MAZIAR NOEI<sup>2</sup> и MASOUD SABERI<sup>3</sup>

<sup>1</sup>Department of Chemical Engineering, Mahshahr Branch, Islamic Azad University, Mahshahr, Iran,

<sup>2</sup>Department of Chemistry, Faculty of Pharmaceutical Chemistry, Tehran Medical Sciences, Islamic Azad University, Tehran, Iran и <sup>3</sup>Department of Chemical Engineering, Bushehr Branch, Islamic Azad University, Bushehr, Iran

Циљ ове студије је развој мешаних матричних мембрана(МММ) на бази силицијум-диоксида MCM-41 диспергованог у полисулфону (PSf) за одвајање угљен-диоксида од метана. У ту сврху MCM-41 је синтетизован хидротермалном методом и модификован је са 3-аминопропилтриетоксисиланом (APTES). SEM, FTIR, BET и XRD анализе коришћене су за карактеризацију модификованих и немодификованих честица. Затим су припремљени различити МММ који садрже PSf са различитим масеним процентима (5, 10, 15 и 20 %) модификованих и немодификованих честица и проучавана је морфологија и структура припремљених мембрана помоћу SEM и XRD анализа. Без обзира на врсту честица, додавање MCM-41 у PSf изазвало је повећање пропусности гасова у поређењу са мембрansom од PSf. Додавање немодификованих честица у PSf матрицу резултирало је неидеалним ефектима, укључујући агломерацију честица и/или стварање међуфазних празнина. МММ са модификованим MCM-41 показали су релативно боље перформансе разdvajaњa у поређењу са МММ са немодификованим MCM-41. Као резултат, МММ PSf са 20 mas. % модификованог MCM-41 показала је значајан пораст селективности угљен-диоксида/метана и вредност селективности достигла је 25,24.

(Примљено 19. фебруара, ревидирано 18. априла, прихваћено 29. априла 2021)

#### REFERENCES

1. J. D. Wind, *PhD Thesis*, University of Texas, Austin, TX, 2002 (<https://repositories.lib.utexas.edu/handle/2152/1048>)
2. R. E. Kesting, A. Fritzsche, *Wiley-Inter.* **36** (1993) 102 (<https://doi.org/10.1002/pi.1995.210360116>)
3. X. Guo, Z. Qiao, D. Liu, C. Zhong, *J. Mat. Chem., A* **7** (2019) 24738 (<https://doi.org/10.1039/C9TA09012F>)
4. S. E. Kentish, C. A. Scholes, G. W. Stevens, *Recent Patent Chem. Eng.* **1** (2008) 52 (<https://www.ingentaconnect.com/content/ben/cheng/2008/00000001/00000001/art00005>)
5. P. Pandey, R. Chauhan, *Prog. Polym. Sci.* **26** (2001) 853 ([https://doi.org/10.1016/S0079-6700\(01\)00009-0](https://doi.org/10.1016/S0079-6700(01)00009-0))
6. M. Saberi, *J. Serb Chem. Soc.* **86** (2021) 341 (<https://doi.org/10.2298/JSC200715046S>)
7. A. Bos, I. G. M. Punt, M. Wessling, H. Strathmann, *Sep. Purif. Technol.* **14** (1998) 27 ([https://doi.org/10.1016/S1383-5866\(98\)00057-4](https://doi.org/10.1016/S1383-5866(98)00057-4))
8. J. D. Wind, C. Staudt-Bickel, D. R. Paul, W. J. Koros, *Ind. Eng. Chem. Res.* **41** (2002) 6139 (<https://doi.org/10.1021/ie0204639>)

9. A. Brunetti, P. Bernardo, E. Drioli, G. Barbieri, Y. Yampolskii, B. Freeman, *Membr. Gas Separ.* **6** (2010) 279
10. P. Bernardo, G. Clarizia, *Eng. Trans.* **32** (2013) 1999 (<https://doi.org/10.3303/CET1332334>)
11. L. M. Robeson, *J. Membr. Sci.* **320** (2008) 390 (<https://doi.org/10.1016/j.memsci.2008.04.030>)
12. J. K. Ward, W. J. Koros, *J. Membr. Sci.* **377** (2011) 75 (<https://doi.org/10.1016/j.memsci.2011.04.010>)
13. T. W. Pechar, S. Kim, B. Vaughan, E. Marand, M. Tsapatsis, H. K. Jeong, C. J. Cornelius, *J. Membr. Sci.* **277** (2006) 195 (<https://doi.org/10.1016/j.memsci.2005.10.029>)
14. E. Karatay, H. Kalıpçılar, L. Yılmaz, *J. Membr. Sci.* **364** (2010) 75 (<https://doi.org/10.1016/j.memsci.2010.08.004>)
15. P. Jha, J. D. Way, *J. Membr. Sci.* **324** (2008) 151 (<https://doi.org/10.1016/j.memsci.2008.07.005>)
16. S. Rafiq, Z. Man, A. Maulud, N. Muhammad, S. Maitra, *Sep. Purif. Technol.* **90** (2012) 162 (<https://doi.org/10.1016/j.seppur.2012.02.031>)
17. A. M. Hillock, S. J. Miller, W. J. Koros, *J. Membr. Sci.* **314** (2008) 193 (<https://doi.org/10.1016/j.memsci.2008.01.046>)
18. M. Junaidi, C. Leo, S. Kamal, A. Ahmad, T. Chew, *Fuel Process.* **112** (2013) 1 (<https://doi.org/10.1016/j.fuproc.2013.02.014>)
19. R. Mahajan, R. Burns, M. Schaeffer, W. J. Koros, *J. Appl. Polym. Sci.* **86** (2002) 881 (<https://doi.org/10.1002/app.10998>)
20. T. T. Moore, R. Mahajan, D. Q. Vu, W. J. Koros, *AICHE J.* **50** (2004) 311 (<https://doi.org/10.1002/aic.10029>)
21. X. Liu, H. Sun, Y. Chen, Y. Yang, A. Borgna, *Microporous Mesoporous Mat.* **121** (2009) 73 (<https://doi.org/10.1016/j.micromeso.2009.01.018>)
22. M. Nekoomanesh, H. Arabi, G. Nejabat, M. Emami, G. Zohuri, *Iran. J. Polym. Sci. Tech. (Persian)*, **21** (2008) 243
23. T. L. Chew, A. L. Ahmad, S. Bhatia, *Adv. Coll. Int. Sci.* **153** (2010) 43 (<https://doi.org/10.1016/j.cis.2009.12.001>)
24. G. R. Nejabat, M. Nekoumanesh, H. Arabi, *Iran. Polym. J.* **19** (2010) 79 (<https://www.sid.ir/en/journal/ViewPaper.aspx?id=167621>)
25. T. Yasmin, K. Müller, *J. Chromat.*, **A 1217** (2010) 3362 (<https://doi.org/10.1016/j.chroma.2010.03.005>)
26. M. Laghaei, M. Sadeghi, B. Ghalei, M. Dinari, *Prog. Org. Coat.* **90** (2016) 163 (<https://doi.org/10.1016/j.porgcoat.2015.10.007>)
27. M. Laghaei, M. Sadeghi, B. Ghalei, M. Shahrooz, *J. Mem. Sci.* **513** (2016) 20 (<https://doi.org/10.1016/j.memsci.2016.04.039>)
28. S. Sorribas, B. Zornoza, C. Téllez, J. Coronas, *J. Membr. Sci.* **452** (2014) 184 (<https://doi.org/10.1016/j.memsci.2013.10.043>)
29. J. Yuan, S. Zhou, G. Gu, L. Wu, *J. Mat. Sci.* **40** (2005) 3927 (<https://link.springer.com/article/10.1007/s10853-005-0714-8>)
30. I. F. Vankelecom, E. Scheppers, R. Heus, J. B. Uytterhoeven, *J. Phys. Chem.* **98** (1994) 12390 (<https://doi.org/10.1021/j100098a038>)
31. Q. Cai, Z. S. Luo, W. Q. Pang, Y. W. Fan, X. H. Chen, F. Z. Cui, *J. Chem. Mater.* **13** (2001) 258 (<https://doi.org/10.1021/cm990661z>)

32. M. Janicke, C. Landry, S. Christiansen, S. Birtalan, G. Stucky, B. Chmelka, *Chem. Mat.* **11** (1999) 1342 (<https://doi.org/10.1021/cm981135v>)
33. A. Jomekian, M. Pakizeh, A. R. Shafiee, S. A. A. Mansoori, *Sep. Purif. Technol.* **80** (2011) 556 (<https://doi.org/10.1016/j.seppur.2011.06.011>)
34. T. C. Merkel, Z. He, I. Pinna, B. D. Freeman, P. Meakin, A. J. Hill, *Macromolecules* **36** (2003) 6844 (<https://doi.org/10.1021/ma0341566>)
35. I. F. Vankelecom, S. van den Broeck, E. Merckx, H. Geerts, P. Grobet, J. B. Uytterhoeven, *J. Phys. Chem.* **100** (1996) 3753 (<https://doi.org/10.1021/jp9526511>).